

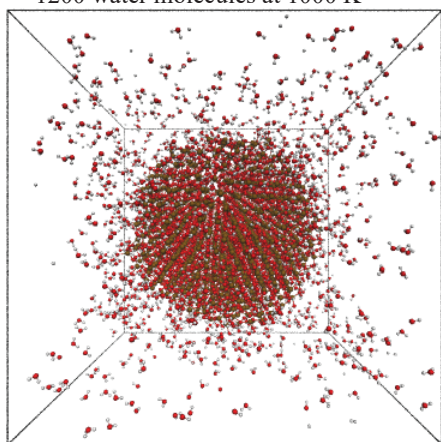
A Reactive Molecular Dynamics Study of Bi-modal Particle Size Distribution in Binder-Jetting Additive Manufacturing using Stainless-Steel Powders

Supplementary Information

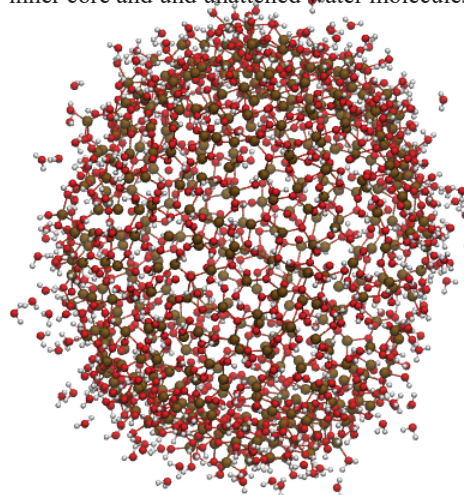
Yawei Gao, Ana Paula Clares, Guha Manogharan, Adri. C.T. van Duin

March 30, 2022

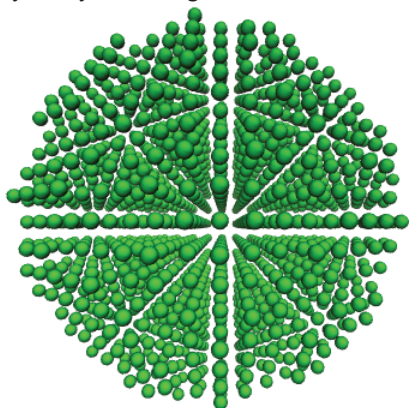
1) Hydrating the particle surface with 1200 water molecules at 1000 K



2) Building the Cr-oxide shell by removing the inner core and und attached water molecules



3) Constructing an iron core from an FCC Fe crystal by truncating the atoms in the corner



4) Assembling the Cr-oxide shell and the iron core to build a core-shell structure.

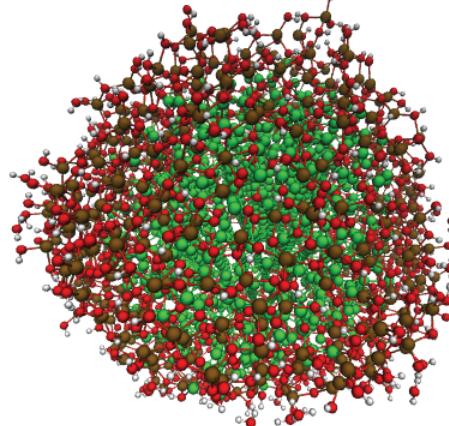
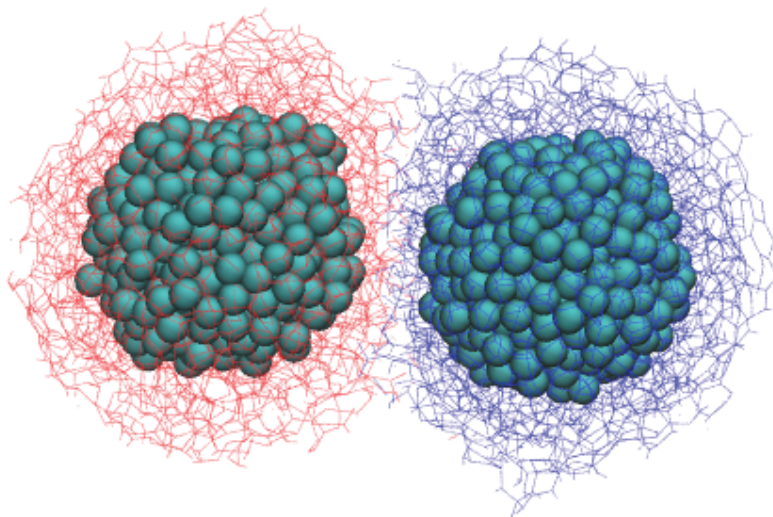


Fig. S1: Procedure of constructing a core-shell particle. Atom colors: Fe (green), Cr (ochre), O (red), and H (white).

(a) Selected atom pairs in the mono-modal particle system



(b) Selected atom pairs in the bi-modal particle system

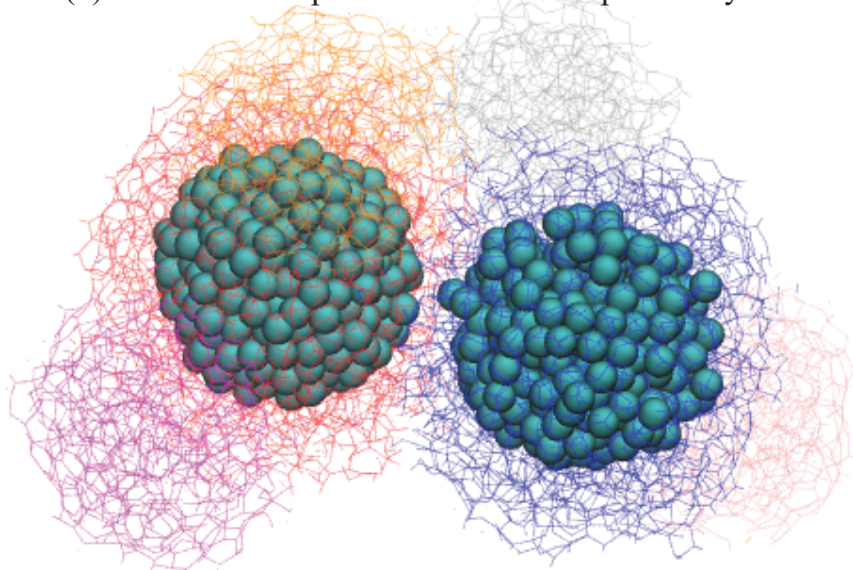


Fig. S2: Selected atom pairs (cyan beads) to assume the restrain energy $E_{\text{restraint}}$. In each coarser particle, the selected atoms form a spherical cluster around the COM with a radius of approximately 13 Å.

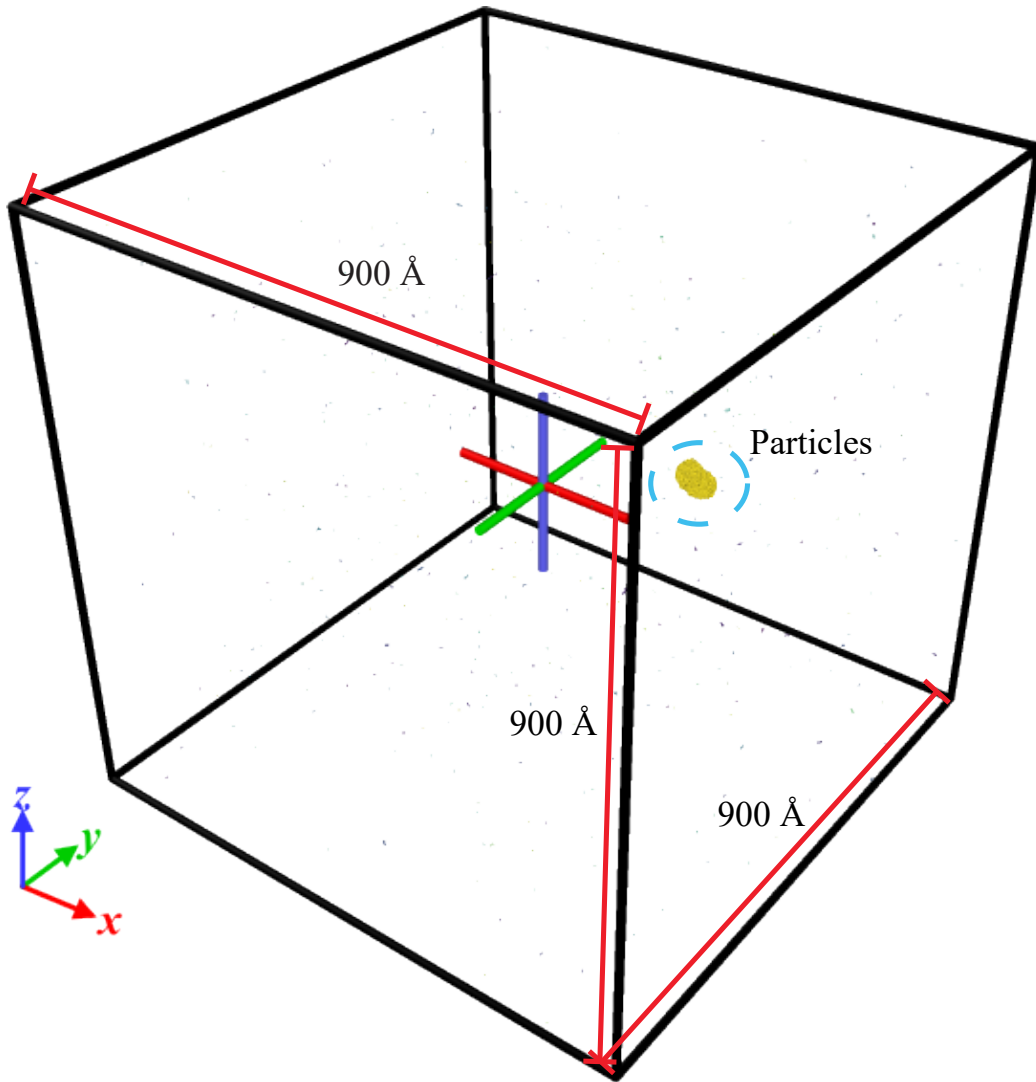


Fig. S3: Snapshot of the mono-modal particle system after 2 ns sintering. The gaseous molecules are scattered far away from the particle cluster. Therefore, their influence on the particles should be limited.

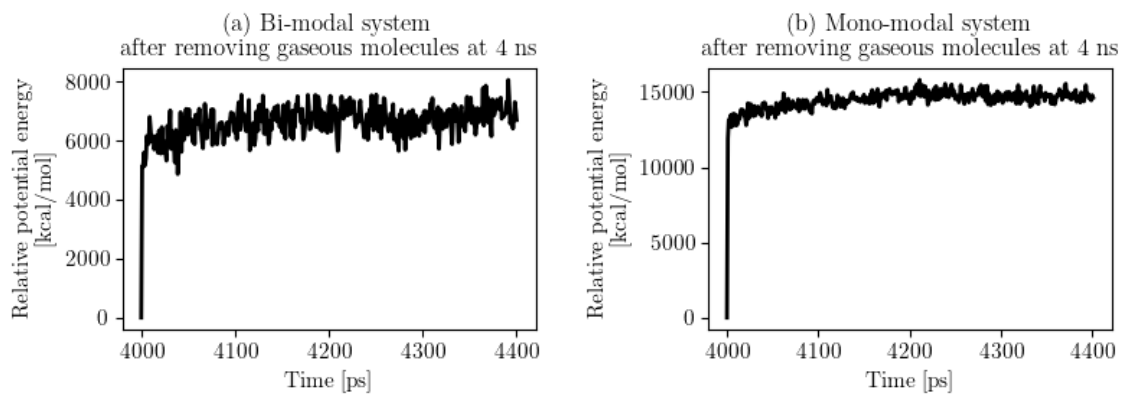
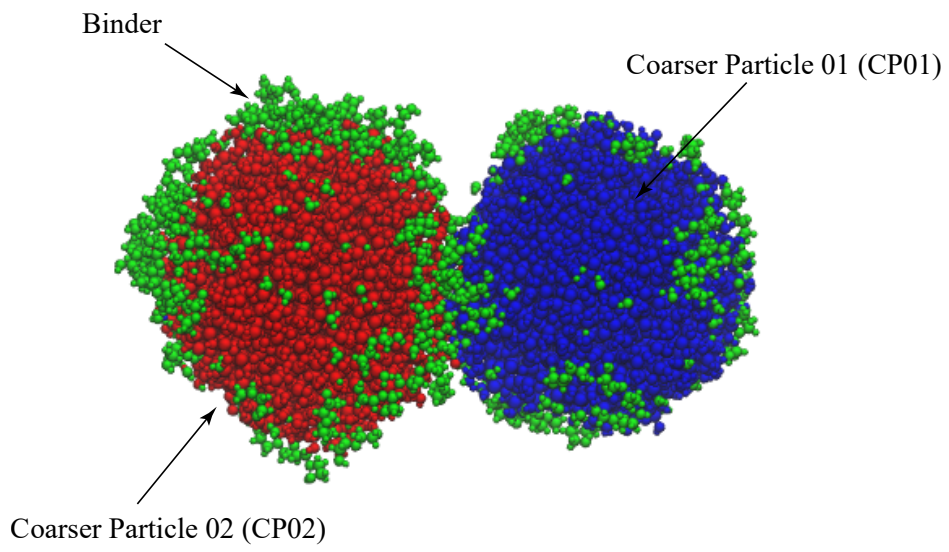
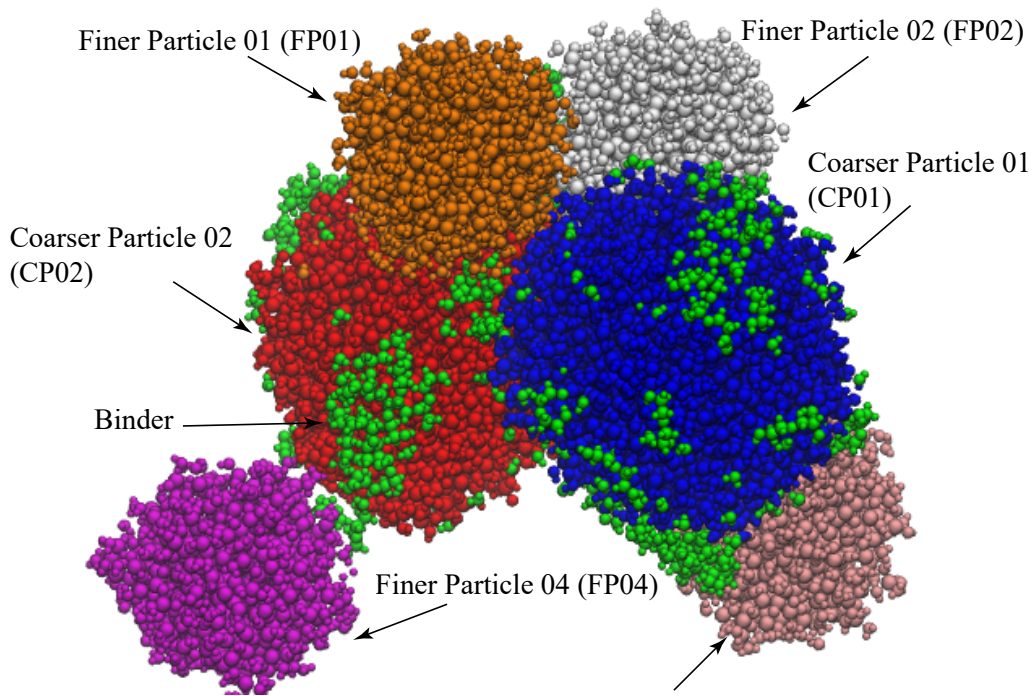


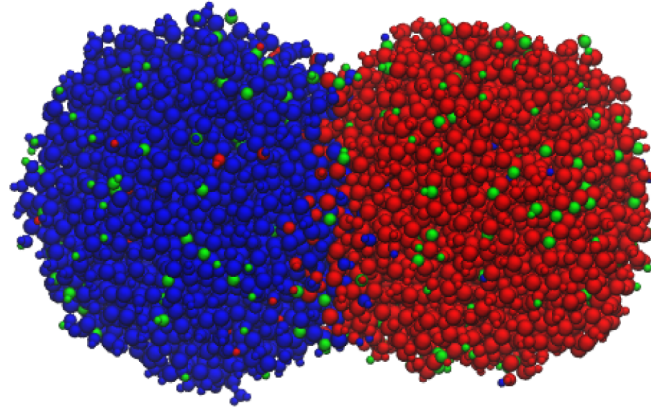
Fig. S4: Potential energy profiles are generally steady after gaseous molecules are removed at time = 4 ns in both the bi-modal (a) and mono-modal (b) particle systems. Hence, the particles at 4 ns should have already reached equilibria.



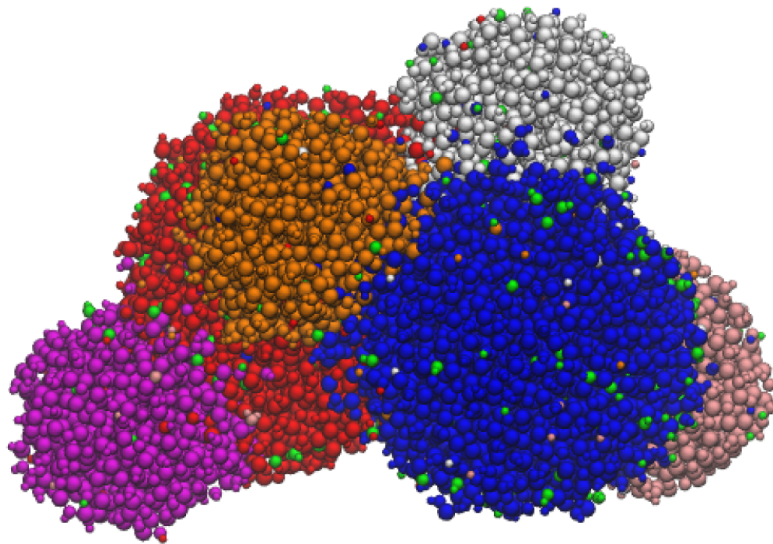
(a) Mono-modal particle system after curing



(b) Bi-modal particle system after curing



(c) Mono-modal particle system after sintering



(d) Bi-modal particle system after sintering

Fig. S5: Bonding of the bi-modal and mono-modal particle systems after curing (a and b), and sintering (c and d). Color scheme: CP01 (blue), CP02 (red), FP01 (orange), FP02 (silver), FP03 (pink), FP04 (magenta), binder (green).

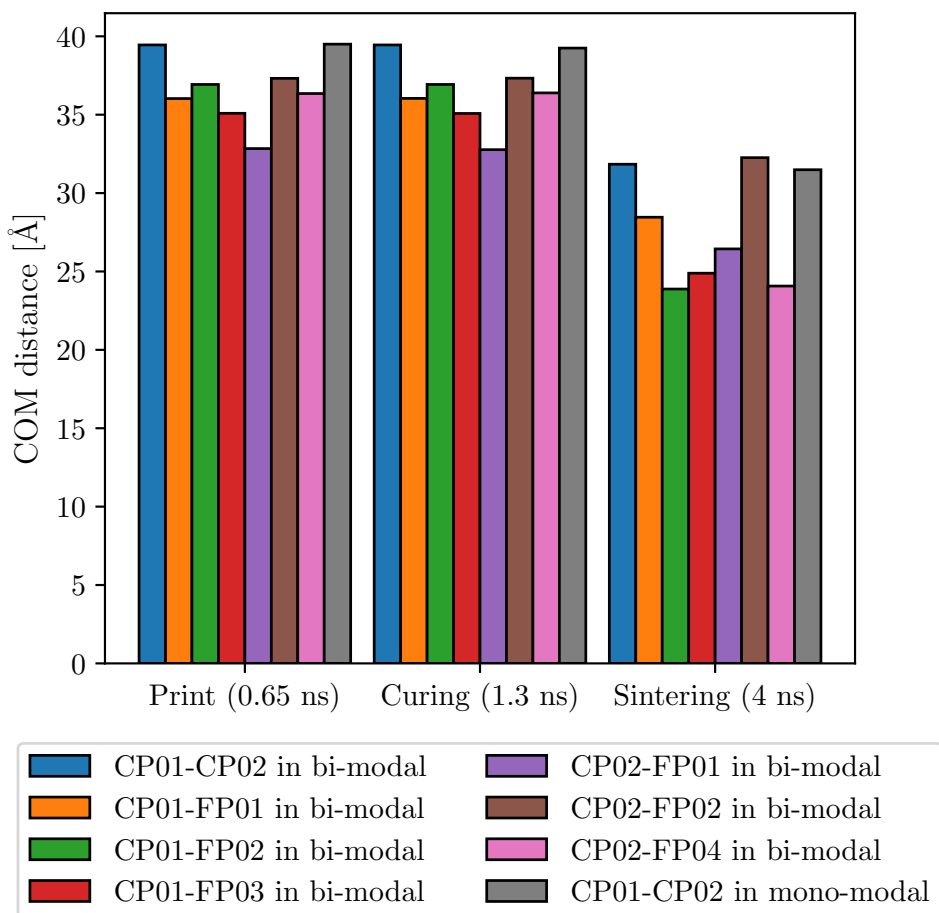


Fig. S6: COM distances among CP01, CP02, FP01, FP02, FP03, and FP04 after print, curing, and sintering. Since CP01/FP04 and CP02/FP03 have no contact, their COM distances are not listed.

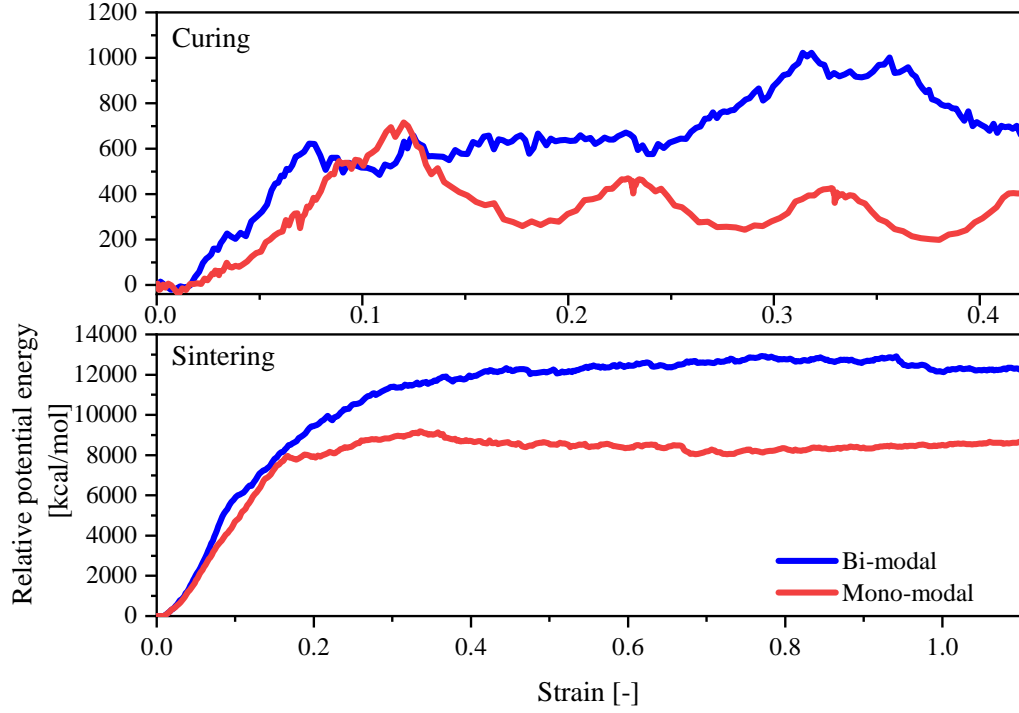


Fig. S7: Relative potential energy profiles of the bi- and mono-modal particle systems subject to an external force field. The potential energy of the equilibrium state is taken as the reference value. It should be noted that the particles merge to an irregular shape that keeps changing during the fracture process. Thus, it is not accurate to quantify the cross-section area and stress. Based on this concern, we use the energy-strain curve instead of the stress-strain curve. The strain $\epsilon = \frac{\Delta d_{\text{com}}}{d_{\text{com},0}} = \frac{d_{\text{com}} - d_{\text{com},0}}{d_{\text{com},0}}$. In this equation, d_{com} is center of mass distance between the coarser particles (CP01 and CP02).

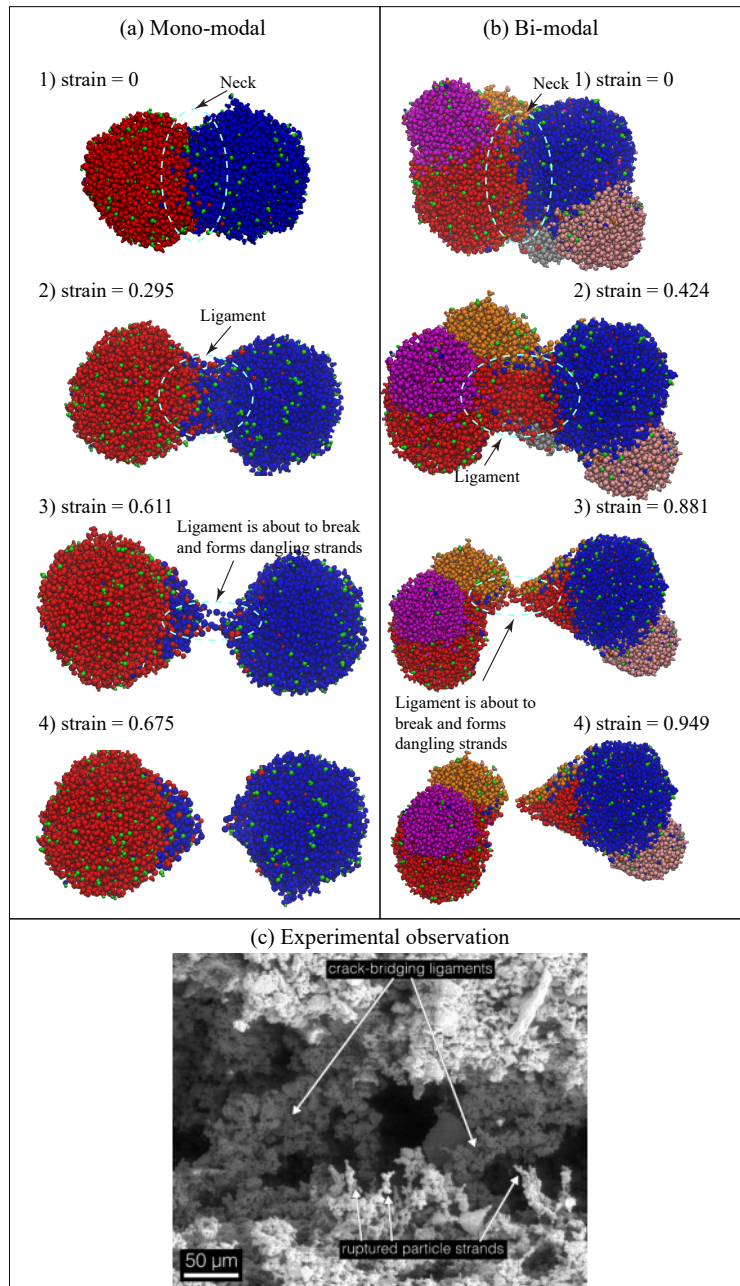


Fig. S8: The ductile fracture processes under an stretching force are similar in the mono-modal (a) and bi-modal (b) particle systems. Color scheme: CP01 (blue), CP02 (red), binder (green), FP01 (orange), FP02 (silver) (FP02 hides behind CP01 and FP01 from this perspective and is therefore only partially visible), FP03 (pink), and FP04 (magenta). (c) Crack-bridging ligaments and ruptured particle strands. Image from Carazzone et al., 2019. [Carazzone *et al.*, *Journal of the American Ceramic Society*, 2019, **102**, 602-610]

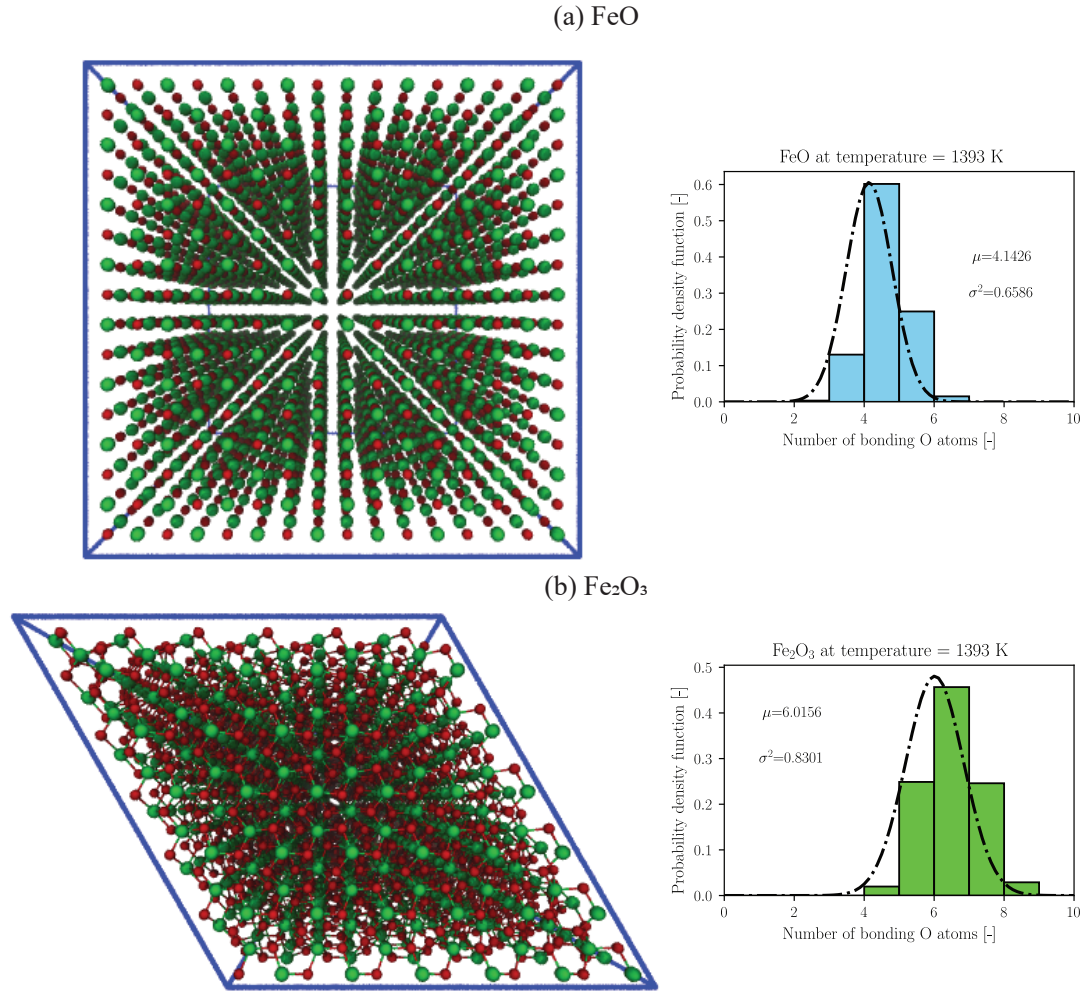


Fig. S9: Probability density functions of O atoms that bond with Fe in FeO and Fe₂O₃, respectively. The FeO supercell is constructed by replicating the cubic unit cell eight times in each Cartesian dimension, while the Fe₂O₃ supercell is constructed by replicating the unit cell six, six, and four times in x , y , z directions, respectively. The FeO and Fe₂O₃ supercells contain 4,096 and 4,320 atoms, respectively. After energy minimization, we perform MD-NPT (The amount of substance (N), pressure (P), and temperature (T) are conserved) at 1393 K for 1 ns (time step = 0.25 fs) with the Berendsen thermostat (temperature damping constant = 100 fs) in each crystal system after geometry optimization. The statistics of O atoms bonding with each reference Fe atom is determined basing on the Fe-O bond order, which are fitted thereafter with a gaussian distribution function independently. More details are referred to the ReaxFF manual [ReaxFF user Manual, 2002] (file fort.7/fort.8).